

ISTITUTO NAZIONALE DI FISICA NUCLEARE  
Laboratori Nazionali di Frascati

LNF-84/69

S.Turck-Chieze et al.: EXCLUSIVE DEUTERON ELECTROINTEGRATION  
AT HIGH NEUTRON RECOIL MOMENTUM

Estratto da:  
Phys. Letters 142B, 145 (1984)

## EXCLUSIVE DEUTERON ELECTRODISINTEGRATION AT HIGH NEUTRON RECOIL MOMENTUM

S. TURCK-CHIEZE, P. BARREAU, M. BERNHEIM, P. BRADU, Z.E. MEZIANI, J. MORGENSTERN  
*Service de Physique Nucléaire — Haute Energie, CEN Saclay, 91191 Gif-sur-Yvette Cedex, France*

A. BUSSIÈRE

*Laboratoire d'Annecy le Vieux de Physique des Particules, Annecy le Vieux, France*

G.P. CAPITANI, E. De SANCTIS

*Laboratori Nazionali di Frascati, Istituto Nazionale di Fisica Nucleare, 00044 Frascati, Italy*

S. FRULLANI, F. GARIBALDI

*Istituto Superiore di Sanità, Laboratorio di Fisica, Rome, Italy  
 and Istituto Nazionale di Fisica Nucleare, Sezione Sanità, Rome, Italy*

and

J. MOUGEY

*Département de Recherche Fondamentale, Laboratoire de Chimie et Physique Nucléaire, 85X 38041 Grenoble Cedex, France*

Received 6 March 1984

We have determined the  $^2\text{H}(\text{e}, \text{e}'\text{p})\text{n}$  cross section for neutron recoil momenta between 295 and 500 MeV/c. In this region the  $^3\text{D}_1$  state contribution is predominant in the deuteron wave function. The high excitation energy ( $E_{\text{cm}}^{\text{np}} = 179$  MeV) and the small momentum transferred ( $q_{\text{cm}}^{-2} = 1.66 \text{ fm}^{-2}$ ) emphasize the influence of isobar configurations (IC). Experimental data are compared with calculations including isobar contributions, mesonic exchange currents and final state interactions.

In the last two decades a great effort has been done to put experimental constraints on the available realistic nucleon–nucleon (N–N) potentials, both to possibly discriminate among several proposed interactions and to elucidate the role of non-nucleonic degrees of freedom in the framework of OBE and derived potentials. In the few-body systems, the non-nucleonic effects are often important and the deuteron, even if it is loosely bound, is one of the best candidates because complete calculations can in principle be performed. Mesonic degrees of freedom have clearly shown up in various electromagnetic processes. In electron scattering, for example, compelling evidence for mesonic exchange currents (MEC) was given by experiments on deuteron electrodisintegration near

threshold [1]. A review of these inclusive experiments and of their interpretation has recently been done by Leidemann and Arenhövel [2]. Isobar contributions (IC) effects have been observed in some photodisintegration experiments [3].

Through the proton angular distribution of the  $^2\text{H}(\text{e}, \text{e}'\text{p})$  experiment it is possible to measure the neutron recoil momentum  $|\text{n}'|$  distribution which, in plane wave impulse approximation (PWIA), is a direct measurement of the deuteron wave function. A few years ago, we performed a measurement up to  $|\text{n}'| = 340$  MeV/c [4] to get information on the poorly known deuteron D state wave function. Nevertheless, final state interactions (FSI) and meson exchange currents (MEC) have to be taken into account in addi-

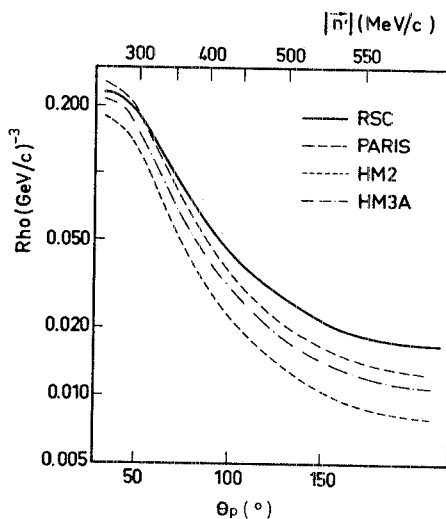


Fig. 1. The deuteron momentum density  $\rho$  [4] defined as

$$\rho(p) = \left| \int u(r) j_0(pr) r dr \right|^2 + \left| \int w(r) j_2(pr) r dr \right|^2$$

for different nucleon-nucleon interaction models: RSC [7], Paris [8], HM2 and HM3a [9]. The D state admixture probability  $P_D$  is respectively 6.47%, 5.77%, 4.32%, 5.18%.  $u(r)$  and  $w(r)$  are the radial wave functions for the S and D states respectively.

tion to the direct knock out. An elaborate theoretical analysis done by Arenhövel [5] is in good agreement with the experimental results.

It is in the momentum region from 300 to 500 MeV/c, where the D-state is dominant [6], that the deuteron wave functions computed from various nucleon-nucleon potentials have the largest differences (fig. 1). To explore this region with reasonable counting rates, it is necessary to perform the measurements at small electron scattering angles. This leads to work at high excitation energy but low momentum transfer, that is in kinematical conditions where the contributions from the  $\Delta$ -isobar exchange current (IC) are quite substantial [5,10].

The experiment was performed using the Saclay ALS accelerator and the two-spectrometers set-up of the HE1 end station [11]. Electrons of 560 MeV were incident on a liquid deuterium target consisting of a 15 mm diameter vertical stainless steel cylinder, of wall thickness 0.02 mm. Electrons, scattered at 25°, were detected in the "900" spectrometer operating at a fixed field corresponding to a momentum of 360

MeV/c. These kinematical conditions give an excitation energy of the neutron-proton pair  $E_{cm}^{np} = 179$  MeV and a transferred momentum  $|q_{cm}|^2 = 1.66$  fm<sup>-2</sup>. Protons were detected in the "600" spectrometer at seven different angles and central energies (cf. table 1) in order to measure the neutron recoil momentum distribution. A scintillation counter array was added in the transverse plane of the proton spectrometer, in order to improve the horizontal angular resolution and the missing energy resolution (the gain was about 30% for the latter).

The target could be filled with either hydrogen or deuterium. Hydrogen ( $ee'$ ) elastic cross section measurements allowed determination of the spectrometer solid angle variations due to the extended target, as a function of the scattering angle. These measurements confirmed previous results obtained by displacing a thin  $^{12}\text{C}$  target along the beam. The relative proton detection efficiency, as a function of the proton energy, was determined by measuring the hydrogen elastic ( $ep$ ) and ( $ee'$ ) cross sections in several kinematical conditions. The results showed a 6% variation between the two extreme values of the detected proton energies. By comparing ( $ee'p$ ) and ( $ee'$ ) elastic cross section values from hydrogen, we were also able to estimate the absolute proton detection and coincidence efficiencies. This renormalization factor was  $1.05 \pm 0.05$ . Elastic scattering measurements on the deuteron, when compared to the data of Simon et al. [12] resulted in a  $1.11 \pm 0.02$  correction factor to the product of detector efficiency and nominal target thickness in the electron arm (there was no local measurement of target density). Therefore the absolute cross sections were obtained by introducing a normalization factor  $K = 1.16$ . The uncertainty on this factor is 7% including uncertainties on dead time and absolute measurement on the proton solid angle. The relative variation of the target thickness, due to pressure or beam intensity variations, was accounted for by measuring the electron single arm yields, the relevant spectrometer having been kept at fixed angle and field during the whole measurement.

The fivefold differential cross section, averaged over the detection phase space can be written as:

$$d^5\sigma/dE'd\Omega_e d\Omega_p = KRN/\Delta E' \Delta\Omega_{ep} N_e N_d ,$$

where  $N_e$  is the number of incoming electrons,  $N_d$  the number of deuteron atoms per cm<sup>2</sup>,  $R$  is the ra-

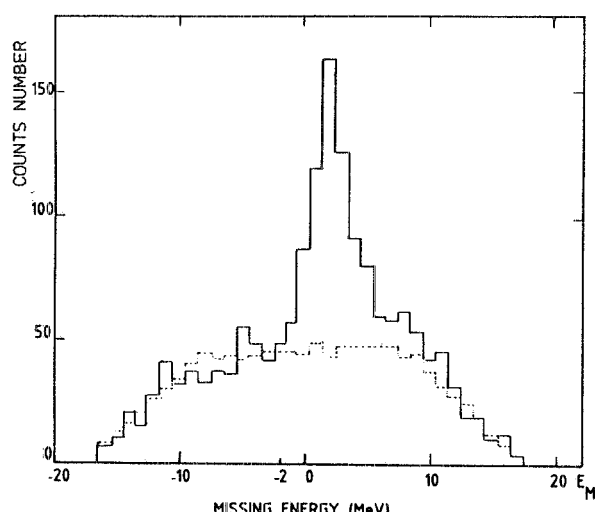


Fig. 2. Missing energy spectrum (full line) for the highest recoil momentum point  $|n'|$  between 480 and 520 MeV/c. Dashed line: accidental events only.

diative correction factor calculated as in ref. [4], and  $N$  is the number of true coincidences.  $\Delta\Omega_{ep}$  is the coincidence solid angle which factorizes, in our geometrical conditions, into the product angular acceptances of the two arms. In the case of  $^2H$ , the kinematics is overdetermined; so the electron momentum acceptance  $\Delta e'$  was matched to the proton momen-

Table 1

Kinematical conditions and experimental results. The kinematical values correspond to values in the center of the acceptances for a coplanar reaction. The error bars are only statistical. An additional 7% uncertainty on absolute normalization must be taken into account.

$E = 560$  MeV,  $E' = 360$  MeV,  $\theta_{e'} = 25^\circ$

$ n' $ (MeV/c)	$\theta_p$ (degrees)	$T_p$ (MeV)	$d^5\sigma/dE'd\Omega_{e'}d\Omega_p$ (pb/MeV sr <sup>2</sup> )
294	46.54	155	182.4 ± 8.2
320	60.41	146.8	162 ± 5.7
340	68.24	140	120.4 ± 5.7
380	82.3	125.5	79.09 ± 3.6
420	96.45	110	45.17 ± 2.8
460	111.93	92.6	33 ± 4.4
500	131.22	74.3	28.4 ± 1.8

tum acceptance in order to avoid coincidence losses. Coincidence time and missing energy resolutions were  $\Delta\tau = 1.5$  ns,  $\Delta E_m \sim 3.0$  MeV; the missing energy spectrum for  $|n'| = 500$  MeV/c is shown in fig. 2. For this point the true coincidence rate was 20 per hour, and the true to accidental ratio was  $\sim 1$ . The beam intensity was kept between 1 and 1.5 microamperes during the whole experiment.

Experimental results are given in table 1. Fig. 3 shows the comparison of our results with Arenhövel's

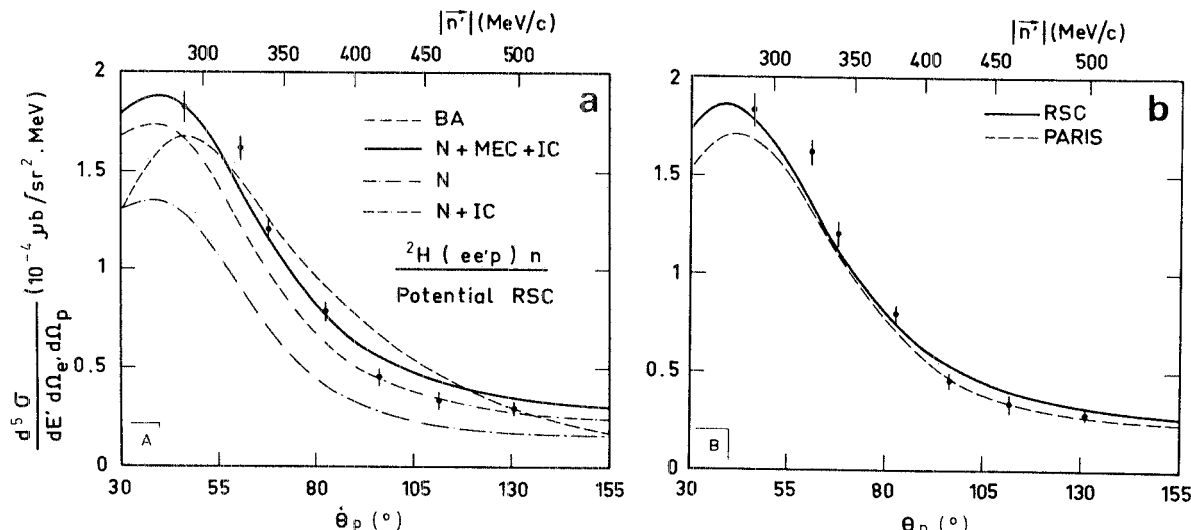


Fig. 3. Experimental results compared with Arenhövel's theoretical calculations [13]. (a) BA: calculation using nucleon plane wave functions,  $N = BA + FSI$ ,  $N + MEC + IC$ : ‘complete’ calculation including explicit meson exchange currents and isobar configurations. (b) Calculation for different potentials (with a reduction of 15% of the M1  $\Delta$ -N transition strength in comparison with (a)).

non relativistic calculation. The BA curve also includes the direct neutron knock-out with detection of the spectator proton. At 500 MeV/c this contribution is of the same order of magnitude as direct proton knock-out. In fig. 3a, the different corrections to BA are shown for the RSC potential [7] ( $P_D = 6.47\%$ ). FSI decrease the cross section by up to 60%, whereas exchange currents increase it by up to a factor of 2 (+65% for IC, +25% for MEC). In spite of the relative compensation of these interaction effects, the Born approximation is clearly insufficient in this kinematics. Nevertheless, there subsists a slight difference between the experimental and theoretical shapes of the angular distributions. This is also the case if other potentials are used, such as the Paris potential [8] ( $P_D = 5.77\%$ ), which better reproduce the high momentum part of the distribution (see fig. 3b). Comparing fig. 1 and fig. 3b one sees a reduction of the difference between the RSC and Paris potential predictions when the complete calculation is performed. One must remark that these two potentials give similar  $P_D$  values. A preliminary calculation by Laget [14], including exchange currents and rescattering effects (in S-wave only), shows significant difference between HM2 [9] ( $P_D = 4.32\%$ ) and RSC [7].

We have measured the deuteron electrodisintegration cross section with an accuracy of  $\sim 10\%$  in a mo-

mentum region where deuteron wave functions computed with realistic N-N potentials differ substantially. Discrimination among some of these potentials might be possible when complete calculations, including relativistic effects, become available.

### References

- [1] R.E. Rand, R.F. Frosch, C.E. Litting and M.R. Yearian, Phys. Rev. Lett. 18 (1967) 469; G.G. Simon et al., Nucl. Phys. A324 (1979) 277; M. Bernheim et al., Phys. Rev. Lett. 46 (1981) 402.
- [2] W. Leidemann and H. Arenhövel, Nucl. Phys. A393 (1983) 385.
- [3] J.M. Laget, Phys. Rep. 69 (1981) 1.
- [4] M. Bernheim et al., Nucl. Phys. A365 (1981) 349.
- [5] H. Arenhövel, Nucl. Phys. A384 (1982) 287.
- [6] J. Mougey et al., Nucl. Phys. A262 (1976) 461.
- [7] R.V. Reid, Ann. Phys. (NY) 50 (1968) 411.
- [8] M. Lacombe et al., Phys. Rev. C21 (1980) 861.
- [9] K. Holinde and R. Machleidt, Phys. Rep. 68 (1981) 121.
- [10] W. Fabian and H. Arenhövel, Nucl. Phys. A314 (1979) 253.
- [11] P. Leconte et al., Nucl. Instrum. Methods 169 (1980) 401.
- [12] G.G. Simon, Ch. Schmitt and V.H. Walther, Nucl. Phys. A364 (1981) 285.
- [13] H. Arenhövel, private communication.
- [14] J.M. Laget, Nucl. Phys. A312 (1978) 265; and private communication.